Current Biology, Vol. 14, 678–684, April 20, 2004, ©2004 Elsevier Ltd. All rights reserved. DOI 10.1016/j.cub.2004.03.035

Glia Engulf Degenerating Axons during Developmental Axon Pruning

Ryan J. Watts,[1] Oren Schuldiner,[1] John Perrino,[3] Camilla Larsen,[4] and Liqun Luo[1,2,*]
[1]Department of Biological Sciences
[2]Neurosciences Program
[3]Cell Sciences Imaging Facility
Stanford University
Stanford, California 94305
[4]National Institute for Medical Research
The Ridgeway Mill Hill
London NW7 1AA
United Kingdom

Summary

Developmental axon pruning is widely used in constructing the nervous system. Accordingly, diverse mechanisms are likely employed for various forms of axon pruning [1–7]. In the *Drosophila* mushroom bodies (MB), γ neurons initially extend axon branches into both the dorsal and medial MB axon lobes in larvae. Through a well-orchestrated set of developmental events during metamorphosis, axon branches to both lobes degenerate prior to the formation of adult connections [6, 8]. Here, we analyze ultrastructural changes underlying axon pruning by using a genetically encoded electron microscopic (EM) marker to selectively label γ neurons. By inhibiting axon pruning in combination with the use of this EM marker, we demonstrate a causal link between observed cellular events and axon pruning. These events include changes in axon ultrastructure, synaptic degeneration, and engulfment of degenerating axon fragments by glia for their subsequent breakdown via the endosomal-lysosomal pathway. Interestingly, glia selectively invade MB axon lobes at the onset of metamorphosis; this increase in cell number is independent of axon fragmentation. Our study reveals a key role for glia in the removal of axon fragments during developmental axon pruning.

Results and Discussion

Ultrastructural Changes as a Consequence of MB γ Neuron Pruning

Axon pruning of *Drosophila* MB γ neurons occurs through a defined set of temporally regulated morphological changes, hallmarked by the fragmentation of axons between 8–12 hr after puparium formation (APF; see Figure 1A; [6, 8]). By expressing a genetically encoded EM marker composed of horseradish peroxidase (HRP) fused to a type I transmembrane protein, CD2, we can label select populations of cells for EM analysis (Figure S1; [9]). By using HRP::CD2 to specifically label membranes of MB γ neurons, we performed a detailed time-course study of developmental axon pruning from late larval stages to the peak of axon degeneration. Fluorescence images shown in Figures $1B_1$–$1E_1$ demonstrate the progressive fragmentation and degeneration of both dorsal (d) and medial (m) axon lobes as described previously [6].

A general change in ultrastructure is already evident at low magnification (Figures $1B_2$–$1E_2$). In third-instar larvae, labeled γ neuron axon profiles (L) form a continuous band surrounded by unlabeled profiles (U) that include α′/β′ axons and postsynaptic targets of MB neurons (Figure $1B_2$). From 8–12 hr APF, labeled profiles (L) are progressively interrupted by unlabeled (U) structures (Figures $1C_2$–$1E_2$). In addition, there appears to be a marked increase in the number of vacuoles adjacent to labeled profiles (v, Figures $1C_2$–$1E_2$). In contrast, axonal peduncles, which do not undergo pruning [6, 8], exhibit little ultrastructural changes (data not shown; see Figure S1). This observation differs from a previous report suggesting removal of MB peduncular axons during early metamorphosis [10].

At higher magnification, we frequently observe labeled profiles of γ neurons that form presynaptic terminals in third-instar larvae (arrowheads in Figure $1B_3$). Later time points reveal signs of synaptic degeneration (arrowheads; compare Figures $1B_3$ and $1E_3$). For instance, some labeled presynaptic terminals are filled with uneven-sized vesicles, including large vesicles (arrowheads, Figure $1E_3$); yet others have very few vesicles and are electron lucent. Analysis of high-magnification micrographs of the border between labeled neurons and unlabeled elements reveal prominent structures, including multivesicular bodies (MVBs) at early time points (arrows, Figures $1C_3$ and $1D_3$) and multilamellar bodies (MLBs) at later time points (asterisks, Figures $1D_3$ and $1E_3$). Although many MVBs and MLBs are labeled by HRP::CD2, indicating that they originate from MB γ neurons, they are found within cellular profiles whose plasma membrane is unlabeled by HRP::CD2 (open arrowheads, Figures $1C_3$–$1E_3$).

To determine whether these ultrastructural changes are a consequence of axon pruning, we inhibited MB γ neuron pruning by expressing a yeast ubiquitin-specific protease (UBP2) in γ neurons [6] and performed EM analysis. We found major differences between EM profiles from MBs of wild-type (Figures 1 and 2A) and UBP2-expressing animals (Figure 2B). At low magnification, a decrease in the number of vacuoles as well as a general decrease in the interruption of labeled axon profiles (L) by unlabeled elements (U) in UBP2-expressing animals is observed (compare Figures $2A_2$ and $2B_2$). Two major morphological differences intrinsic to labeled axons are evident at higher magnification. First, the microtubule cytoskeleton appears to be absent or disrupted in wild-type γ axons from 6–12 hr (arrows, Figure $2A_3$; 6 hr data not shown), consistent with previous studies at the light microscope level [6]; however, in UBP2-expressing neurons, axons maintain a readily identifiable microtubule cytoskeleton even at 12 hr APF (arrows, Figure $2B_3$). Second, in wild-type animals, both the length and diameter of axons appear to decrease during pruning, with long axon profiles rarely observed at 12 hr APF; however, in UBP2-expressing γ neurons, many long axon profiles

*Correspondence: lluo@stanford.edu

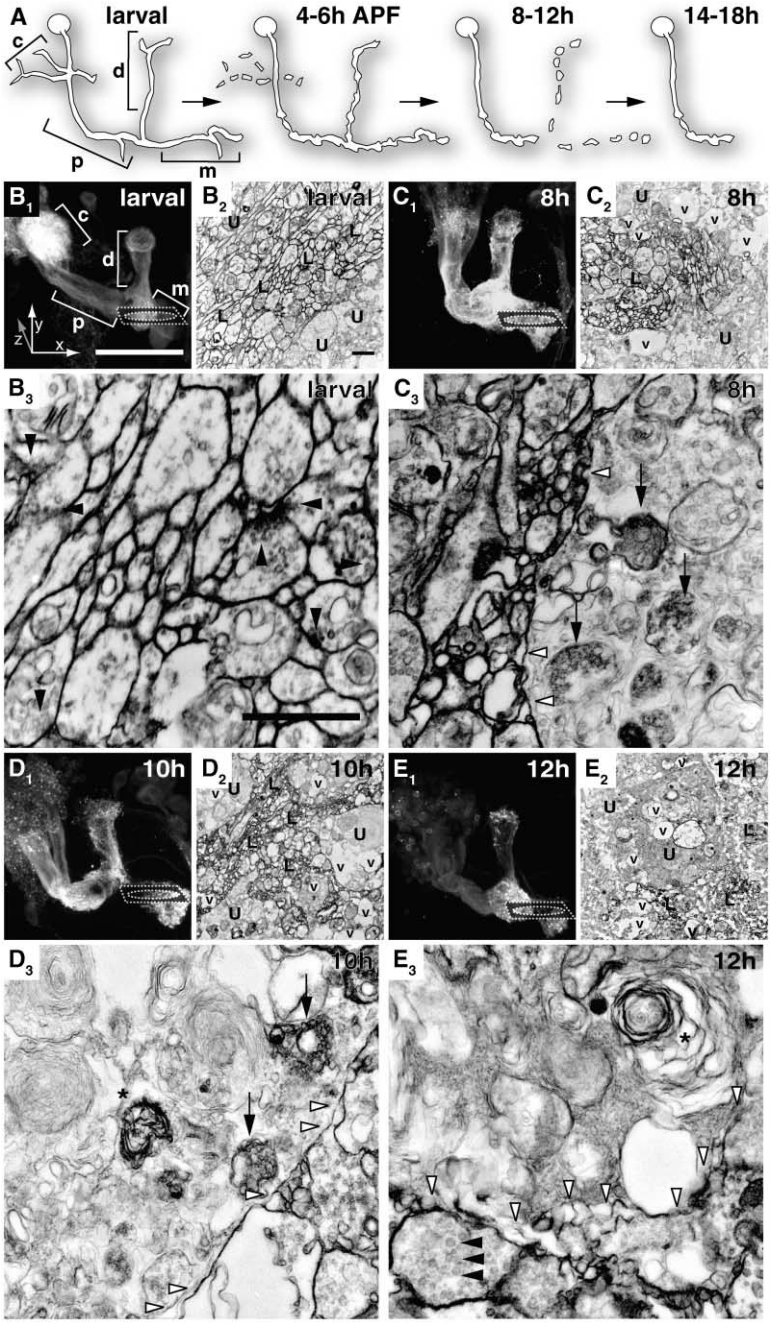

Figure 1. Ultrastructural Time-Course Analysis of Axon Pruning

(A) Schematic illustration of developmental axon pruning of MB γ neurons. Larval γ neurons consist of dendrites near the cell body in the calyx (c) and axons that extend down the peduncle (p) and branch to form the dorsal (d) and medial (m) axon lobes. 4–6 hr after puparium formation (APF), dendrites begin to fragment and axons begin to swell. From 8–12 hr APF, axons in dorsal and medial lobes undergo fragmentation while dendrite fragments disappear. The remaining axon fragments disappear from 14–18 hr APF [6,8]. In this schematic and all light microscopic figures in this paper, the left MB is shown, with dorsal up and midline to the right.

(B–E) Analysis of axon degeneration and ultrastructural changes during axon pruning at different developmental time points: larval MB (B), 8 hr (C), 10 hr (D), and 12 hr (E) APF. (B_1–E_1) Confocal Z projections of MB γ neurons expressing UAS-mCD8::GFP driven by 201Y-GAL4, with labeling of dendrites in the calyx (c); axon bundle or peduncle (p); and axon lobes, medial (m) and dorsal (d). Dashed boxes show the approximate location of longitudinal sections through the medial lobe where EM images were taken.

(B_2–E_2) 15,000× and (B_3–E_3) 40,000× digital electron micrographs of developing MB γ neurons expressing UAS-HRP::CD2 driven by 201Y-GAL4. Labeled profiles are marked with (L), unlabeled with (U), vacuoles with (v), arrowheads mark synaptic terminals, and arrows and asterisks indicate labeled multivesicular bodies (MVBs) and multilamellar body (MLB), respectively, in an otherwise unlabeled cellular profile marked by open arrowheads. Because unlabeled membranes are sometimes juxtaposed with labeled membranes, the extramembraneous nature of the HRP::CD2 marker makes the unlabeled profiles appear interrupted by labeled segments. Genotype: *y,w;UAS-HRP::CD2,UAS-mCD8::GFP,201Y-GAL4/+*.

Scale bar: 50 μm in B_1–E_1, and 1 μm in B_2–E_2 and B_3–E_3.

with wider diameters persist (compare Figures $2A_3$ and $2B_3$).

The most striking differences between wild-type and UBP2-expressing MBs is the prevalence of MVBs and MLBs. When axon pruning is inhibited, the frequency of MLBs is greatly reduced (Figure 2C). Interestingly, the number of unlabeled MLBs remains unchanged, while there is at least a 4-fold decrease in the number of labeled MLBs when pruning is inhibited (e.g., compare Figures $1C_3$, $1D_3$, and $2A_4$ to Figure $2B_4$; quantified in Figure 2C).

Thus, the major ultrastructural changes we have described so far are a direct consequence of axon pruning. In particular, we were struck by the presence of labeled axon profiles within MVBs and MLBs of seemingly extrinsic cells, and the dependence of these external MVBs and MLBs on γ neuron axon pruning. Given that MVBs and MLBs are usually associated with the endosomal-lysosomal pathway (e.g., [11, 12]), the simplest hypothesis is that these structures reflect the uptake of degenerating axons by extrinsic cells for lysosomal-mediated degradation.

Degenerating Axons Are Engulfed by Glia

The cytoplasm of the extrinsic cells harboring MVBs and MLBs have the characteristic punctate labeling reminiscent of rosette-patterned arrays of glycogen granules typically found in glia (see the electron dense cytoplasm

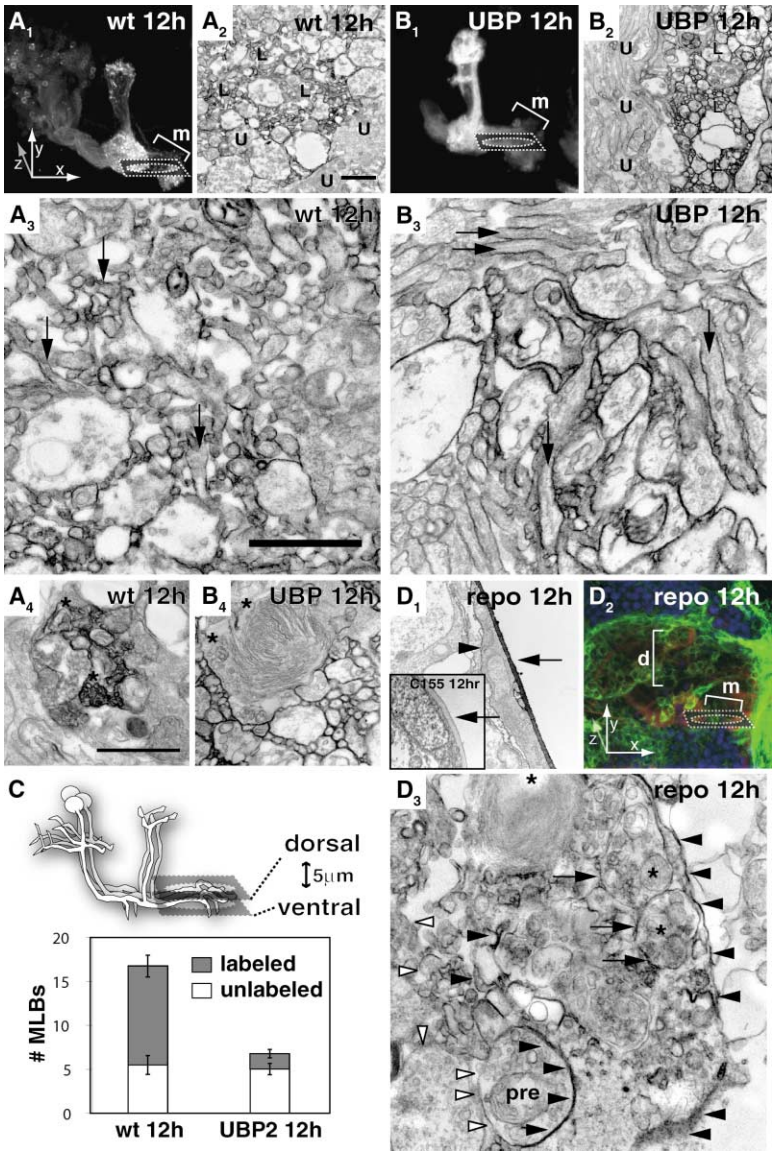

Figure 2. Ultrastructural Comparisons of Wild-type and UBP2-Expressing Axons

(A_1 and B_1) Confocal Z projection of 201Y-GAL4 driving mCD8::GFP. Dashed boxes show approximate location of longitudinal sections through the medial lobe that were processed for EM. 25,000× (A_2 and B_2), 40,000× (A_3 and B_3), and 60,000× (A_4 and B_4) digital electron micrographs of labeled medial lobe by using 201Y-GAL4 to drive expression of HRP::CD2. Genotype: Wild-type (A), same as in Figure 1; UBP2-expressing (B), *y,w;UAS-HRP::CD2,UAS-mCD8::GFP,201Y-GAL4/UAS-UBP2*.

(C) Quantification of labeled and unlabeled MLBs. Illustration defines region from which sections were taken for quantification. n = 4 for each genotype. Error bars represent the standard error of the mean for labeled and unlabeled MLBs.

(D_1) Ultrastructural analysis of labeled glia, 15,000× digital micrograph of repo-GAL4 driving expression of HRP::CD2 labeling surface glia (arrowhead), and perineurium (arrow) at the edge of the brain (D_1). Genotype: *y,w;UAS-HRP::CD2/+;repo-GAL4/+*. Inset: 15,000× digital micrograph of pan-neural C155-GAL4 driving expression of HRP::CD2 labeling neuron cells bodies, but not perineurium (arrow). Gentoype: *y,w,C155-GAL4/y,w;UAS-HRP::CD2/+*.

(D_2) Confocal Z projection taken from Figure 3D, with the dashed box showing section orientation for EM image in (D_3).

(D_3) 40,000× image of labeled glial profile (arrowheads) with unlabeled MVBs and MLBs (asterisks) and unlabeled axon and synaptic profiles (open arrowheads). Genotype as in (D_1). Scale bar: 1 μm for all EM panels.

within unlabeled profiles marked by open arrowheads, Figure 1; e.g., [13, 14]). To begin testing the hypothesis that glia are responsible for engulfing axon fragments during developmental axon pruning, we first examined whether glia are adjacent to the degenerating dorsal and medial MB lobes during early pupal stages. By labeling neuronal nuclei with anti-Elav [15] and glial nuclei with anti-Repo [16, 17], we found that all nuclei (as visualized by a DNA staining) in the vicinity of the MB lobes are either neuronal or glial at all stages examined (data not shown; Figure 3B). In particular, the degenerating medial lobe in the central brain neuropil is surrounded only by glial nuclei (Figure 3B).

By using repo-GAL4 to drive expression of membrane bound mCD8::GFP, we found an increase of glial membrane labeling surrounding both the dorsal (Figures $3C_1$–$3D_1$) and medial (Figures $3C_2$–$3D_2$) lobes during the time of axon degeneration. These glial membranes appear to infiltrate into the axon lobes as axon pruning progresses (arrows, compare Figures $3C_2$ and $3D_2$). We confirmed that the cells surrounding the degenerating lobes are glia by using additional glial markers including mCD8::GFP driven by gcm-GAL4-marking glia [18, 19] and immunolocalization of Draper [20] (data not shown).

To determine whether glia are the extrinsic cells that harbor labeled degenerating axons in the form of labeled MVBs and MLBs (Figures 1 and 2A–2C), we labeled glial membranes by expressing HRP::CD2 with repo-GAL4 to study the pruning process by using EM. As a positive control, we verified that we can label a previously characterized population of glia on the surface of the brain [14, 21] (arrowhead, Figure $2D_1$). We next examined glia in the region of degenerating MB lobes at 12 hr APF. Figure $2D_2$ is a fluorescence image highlighting the end of the medial lobe (dashed box) where EM sections were taken. Figure $2D_3$ shows a typical example. In contrast to the EM micrographs shown in Figures 1, 2A, and 2B, small axon profiles and synapses are no longer labeled (open arrowheads). On the other hand, the plasma membrane of large profiles containing numerous MVBs,

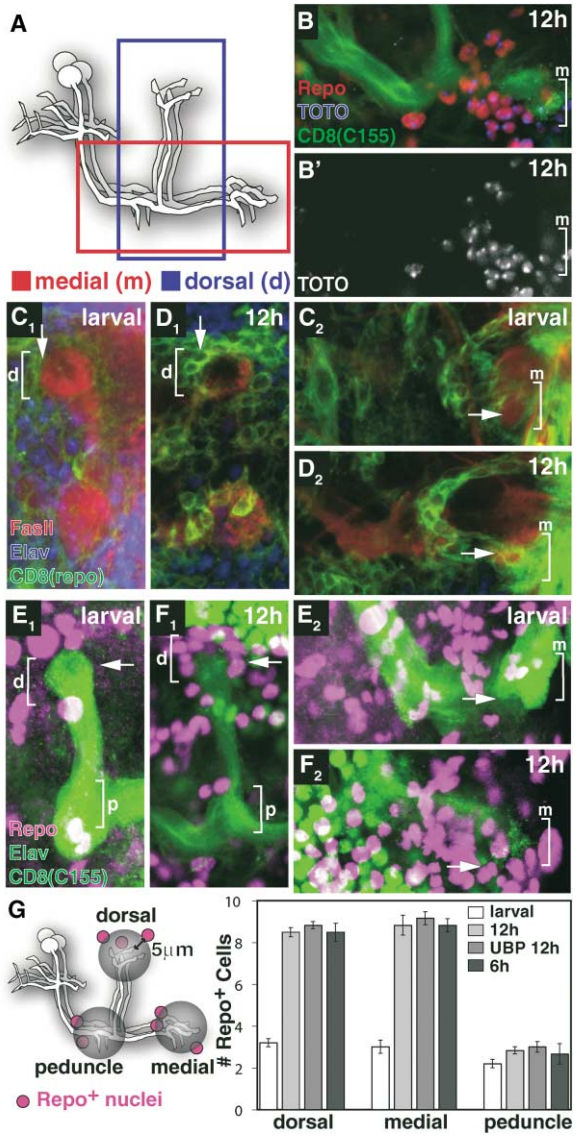

Figure 3. Glia Distribution in MB Axon Lobes during Pruning

(A) Schematic diagram representing image panel orientation.

(B) Image of the medial lobe triple stained with anti-Repo (red), labeling glia nuclei; TOTO (blue), labeling all nuclei; and anti-CD8 (green), labeling mCD8::GFP expressed under the control of a pan-neural *C155-GAL4*. Only the TOTO labeling is shown in (B′). Genotype: *y,w,C155-GAL4/y,w;UAS-mCD8::GFP/+*.

(C and D) Larval (C) or 12 hr APF (D) brains triple stained with anti-FasII (red), labeling γ neurons; anti-Elav (blue), labeling neuronal nuclei; and anti-CD8 (green), labeling mCD8::GFP expressed under the control of repo-GAL4. As a control for the population of cells that repo-GAL4 labels, we also expressed nuclear GFP with repo-GAL4; labeling recapitulates anti-Repo antibody staining (data not shown). Genotype: *y,w;UAS-mCD8::GFP/+;repo-GAL4/+*.

(E and F) Larval (E) or 12 hr APF (F) brains double stained with anti-Repo (magenta), labeling glial nuclei; and anti-CD8 (green), labeling mCD8::GFP expressed under the control of C155-GAL4. Genotype: *y,w,C155-GAL4/y,w;UAS-mCD8::GFP/+*. Arrows indicate analogous locations in the dorsal (E_1 and F_1) or medial (E_2 and F_2) lobes for comparison.

(G) Quantification of the number of Repo-positive nuclei within 5 μm of the dorsal lobe, medial lobe, or the peduncle, as defined by the illustration on the left. Permutation test was done comparing wt larval (n = 5) with either wt at 6 hr or 12 hr or UBP at 12 hr (n = 6 for all three conditions) in both the dorsal and medial lobes ($p < 0.003$ for each comparison, 10,000 repetitions). The same comparison of data collected around the peduncle showed no significant difference. Error bars represent the standard error of the mean. See the Supplemental Experimental Procedures for details.

MLBs, and glycogen granules are labeled by HRP::CD2 (arrowheads), verifying their glial identity. Consistent with the hypothesis that MVBs and MLBs contain axon fragments engulfed by glia, none of the small profiles within the MVBs and MLBs are labeled by HRP::CD2 (asterisks). In contrast, some of the intracellular membranes that surround the MVBs and MLBs are labeled with HRP::CD2 (arrows). Additionally, in this representative electron micrograph there appears to be an unlabeled presynaptic terminal (pre) in the process of being engulfed by the labeled glial profile (pre, Figure $2D_3$).

The results from these complementary EM studies, in which HRP::CD2 selectively labels either MB γ axons (Figures 1 and 2A-C) or glia (Figure 2D), strongly support the hypothesis that MVBs and MLBs are the consequence of engulfment of degenerating axons by glia through a phagocytic process.

Extensive Lysosomal Activity in Glia Associated with Axon Pruning

MVBs and MLBs are typically thought to be associated with the endosomal-lysosomal pathway, which plays an important role in degradation of engulfed proteins and cellular debris (reviewed in [22, 23]). Specifically, studies of the endosomal-lysosomal pathway in *Drosophila* have implicated MVBs and MLBs in the breakdown of engulfed proteins (e.g., [12, 24]). To test whether engulfed axon fragments in the form of labeled MVBs and MLBs are degraded via the endosomal-lysosomal pathway, we visualized the distribution of lysosomal compartments by using LysoTracker (Molecular Probes), a vital dye used to stain live samples for acidic organelles.

In wild-type animals, LysoTracker staining at the MB lobes progressively increases during metamorphosis to reach a peak at 10–12 hr APF, concomitant with the degeneration of MB γ axons (Figure 4A). However, when pruning is inhibited in UBP2-expressing MBs, there appears to be a decrease in both the frequency and size of LysoTracker-positive spots (Figure 4B). Quantification (see Experimental Procedures) revealed a 2-fold decrease in total LysoTracker staining in UBP2-expressing brains (Figure 4C). In addition, the general size of LysoTracker-positive spots is dramatically reduced, and the considerable overlap in GFP and LysoTracker staining observed in wild-type is eliminated in UBP2-expressing MBs (compare arrowheads in Figures 4D and 4E). These results indicate that a significant fraction of the increase in LysoTracker staining is a direct consequence of γ axon pruning. The residual staining in UBP2-expressing brains could be attributed to incomplete inhibition of γ axon pruning by UBP2 expression, and the pruning of other neuronal processes (e.g., putative postsynaptic partner of γ neurons) in the vicinity of the MB. The latter explanation could also account for the unlabeled MVBs and MLBs present in EM micrographs when pruning is inhibited (e.g., Figure $2B_4$; Figure 2C).

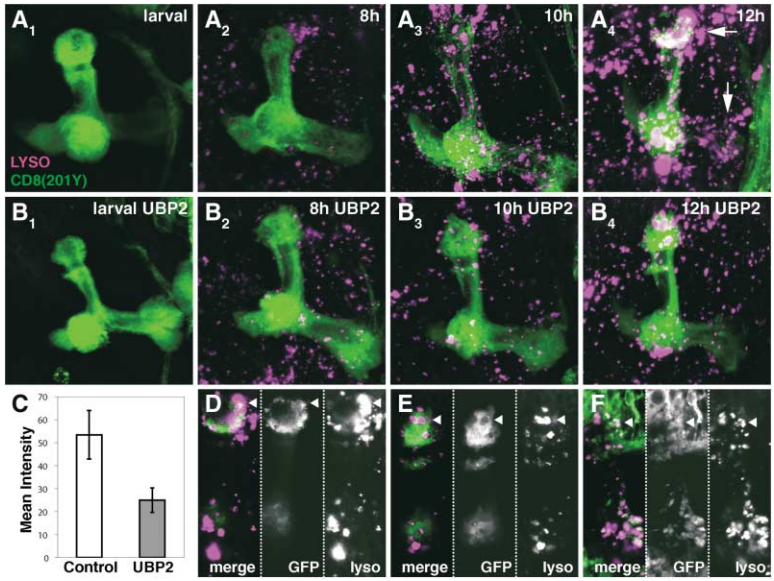

Figure 4. Increase of Lysosomal Activity during Axon Pruning

(A and B) Confocal Z projections of wild-type (A) and UBP expressing (B) MBs at different developmental time points double labeled for γ neurons (green) and LysoTracker (magenta). Genotype: (A) same as in Figure 1; (B), *y,w;UAS-mCD8::GFP,201Y-GAL4/UAS-UBP2*.

(C) Quantification of the mean intensity of LysoTracker labeling comparing wild-type and UBP2-expressing MBs at 12 hr APF (n = 4 for each genotype). This experiment was repeated three times with similar results (result from one experiment is shown). Error bars represent the standard error of the mean.

(D and E) 12 hr APF single optical section through the dorsal lobe showing MB γ axons alone (GFP), LysoTracker alone (lyso), or together (merge). Samples were from wild-type MBs ([D]; genotype as in [A]) or UBP2-expressing MBs ([E]; genotype as in [B]). (D) and (E) were single optical sections taken from the stacks projected in (A_4) and (B_4), respectively.

(F) Single optical section through the dorsal lobe at 12 hr APF showing glial membranes alone (GFP), LysoTracker alone (lyso), or both (merge). Genotype: *y,w;UAS-mCD8::GFP/+; repo-GAL4/+*.

Finally, we find colocalization of glial processes and LysoTracker labeling (arrowheads, Figure 4F), supporting the notion that late endosomal-lysosomal compartments are mainly housed within glia responsible for degradation of engulfed axon fragments.

Glial Invasion of Degenerating Axons Independent of Axon Fragmentation

In the process of studying glial distribution near degenerating lobes, we observed an increase in glial cell bodies as pruning progresses (arrows, compare Figures 3C$_1$ and 3D$_1$). To explore this finding quantitatively, we counted the number of glial nuclei within 5 μm of the tips of both axon lobes and from the end of the peduncle of third-instar larvae and 12 hr APF MBs (compare Figures 3E and 3F; quantified in Figure 3G). We found an approximate 3-fold increase in the number of glial nuclei surrounding the degenerating axons in both the dorsal and medial lobes. However, the number of glia near the peduncle, a region in which axons are not pruned, only increases slightly from third instar to 12 hr APF (Figure 3G).

This selective glial invasion into the degenerating lobes raises an interesting question about the relationship between axon degeneration and glial invasion. Does axon fragmentation induce glial invasion? To address this question, we compared the relative timing of axon degeneration and glial invasion. We found that glial nuclei have already surrounded the axon lobes by 6 hr APF (Figure 3G) before the first sign of axon fragmentation around 8 hr APF [6]. In addition, glial invasion is unaffected when axon pruning is inhibited by UBP2 expression in MB γ neurons (Figure 3G).

Taken together, these results indicate that the specific increase of glial number near degenerating lobes, be it through proliferation or migration, is not triggered by axon degeneration. This finding suggests that glia are not simply reactive to axon fragmentation during developmental axon pruning and raises the interesting possibility that glia may play an instructive role in triggering axon fragmentation. Although axon pruning clearly requires a cell-autonomous genetic program [6, 25], signals from extrinsic cells may provide spatial cues and may assist in the execution of the intrinsic program. A role has also been demonstrated for engulfing cells to assist the cell-intrinsic program of apoptosis [26]. Future genetic manipulations of glia will shed light on the functions of glia-axon interaction during developmental axon pruning.

Conclusions

By using a genetically encoded EM marker to distinguish MB γ neurons and their environment, we have been able to describe pruning events at the ultrastructural level and have advanced our understanding of this developmental process by identifying glia as extrinsic cells important for axon pruning (Figure 5). Glia play numerous roles in the development and function of the nervous system. They are also implicated in engulfing apoptotic cell bodies or neuronal processes during development and degeneration of vertebrate and invertebrate nervous systems, including developmental axon pruning and insect metamorphosis (e.g., [13, 20, 27–30]; reviewed in [31–33]). Our findings add two advances to this vast body of literature. First, we were able to follow a defined population of neurons (MB γ neurons) at both the light- and electron-microscopy level, unequivocally demonstrating that the material glia engulf are from degenerating axons undergoing developmental axon pruning rather than debris from apoptotic cells. Second, the ability to inhibit axon pruning allowed us to demonstrate that many observed phenomena are a direct conse-

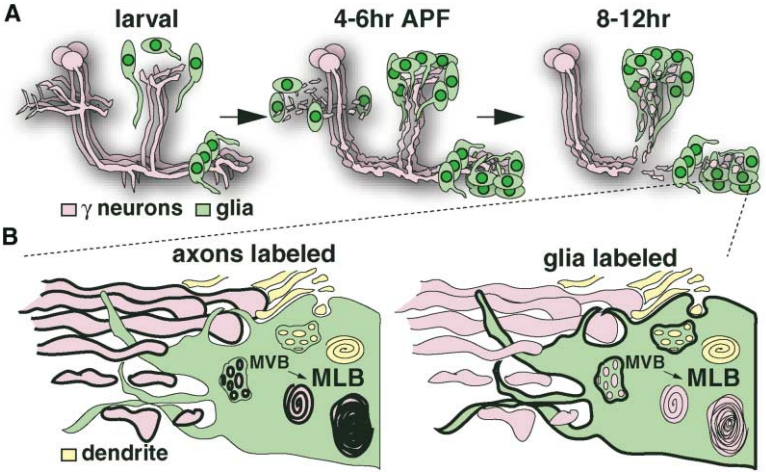

Figure 5. Model for the Role of Glia in Axon Pruning

(A) Schematic diagram summarizing our current model for developmental axon pruning in *Drosophila* MBs incorporating studies of both fluorescence and electron microscopy. Larval MBs are surrounded by several glia in both the dorsal and medial lobe. Beginning around 4–6 hr APF, the number of glia surrounding the dorsal and medial lobe increases 3-fold. Changes in glial number coincide with blebbing of axons and fragmentation of dendrites. From 8–12 hr APF, signs of axon fragments in glial profiles are readily apparent in EM, coincident with axon fragmentation seen by using fluorescent microscopy.

(B) Summary of glial-axon interaction during engulfment stage of developmental axon pruning. Axons labeled: labeled MVBs and MLBs are present within otherwise unlabeled glial profiles. Interestingly, in the same cellular profiles we also observe unlabeled MVBs and MLBs, which we hypothesize to represent unlabeled dendrites from neurons postsynaptic to MB axons. Glia labeled: no MVBs or MLBs are labeled; however, glial plasma membrane and the outer membrane of MVBs are labeled. This suggests that MVBs originate from endocytosis or phagocytosis by glia. Notably, the membrane surrounding MLBs lacks strong labeling in either paradigm. This is likely because MLBs represent a late stage in the endosomal-lysosomal pathway and may therefore originate from lysosomes, which may not include HRP::CD2-labeled plasma membrane on their outermost membrane. Dendrites from putative postsynaptic partners of MB γ neurons are in light yellow; abbreviationis: MVB, multivesicular body; and MLB, multilamellar body.

quence of developmental axon pruning. These phenomena include intrinsic changes of axonal ultrastructures, engulfment of axon fragments by glia, and an increase of lysosomal activity during axon degeneration. In a companion manuscript, Awasaki and Ito [34] provide complementary evidence for the function of glia in axon breakdown during axon pruning. They demonstrate that transient disruption of glial function arrests axon pruning, suggesting an instructive role for glia in developmental axon pruning. Taken together, these studies provide the framework to further investigate the mechanisms underlying axon-glia interactions during developmental axon pruning.

Supplemental Data

Supplemental Data including Figure S1, which describes the genetically encoded EM marker, and detailed Experimental Procedures are available at http://www.current-biology.com/cgi/content/full/14/8/678/DC1/.

Acknowledgments

We thank J.-P. Vincent for generously providing the UAS-HRP::CD2 transgene generated in his laboratory prior to publication. We thank T. Awasaki and K. Ito for communication of unpublished results. We thank S. McConnell, B. Barres, E. Hoopfer, A. Penton, E. Marin, and D. Berdnik for critical comments on our manuscript; and M. Cohen and G.S.X.E. Jefferis for help with statistical analysis. R.J.W. and O.S. receive support from a NRSA predoctoral fellowship and EMBO long-term fellowship, respectively. This work was supported by an NIH grant (R01-NS41044).

Received: January 5, 2004
Revised: February 10, 2004
Accepted: February 10, 2004
Published: April 20, 2004

References

1. Truman, J.W. (1990). Metamorphosis of the central nervous system of Drosophila. J. Neurobiol. *21*, 1072–1084.
2. O'Leary, D.D.M., and Koester, S.E. (1993). Development of projection neuron types, axon pathways, and patterned connections of the mammalian cortex. Neuron *10*, 991–1006.
3. Weimann, J.M., Zhang, Y.A., Levin, M.E., Devine, W.P., Brulet, P., and McConnell, S.K. (1999). Cortical neurons require Otx1 for the refinement of exuberant axonal projections to subcortical targets. Neuron *24*, 819–831.
4. Walsh, M.K., and Lichtman, J.W. (2003). In vivo time-lapse imaging of synaptic takeover associated with naturally occurring synapse elimination. Neuron *37*, 67–73.
5. Bagri, A., Cheng, H.J., Yaron, A., Pleasure, S.J., and Tessier-Lavigne, M. (2003). Stereotyped pruning of long hippocampal axon branches triggered by retraction inducers of the semaphorin family. Cell *113*, 285–299.
6. Watts, R.J., Hoopfer, E.D., and Luo, L. (2003). Axon pruning during *Drosophila* metamorphosis: evidence for local degeneration and requirement of the ubiquitin-proteasome system. Neuron *38*, 871–885.
7. Kantor, D.B., and Kolodkin, A.L. (2003). Curbing the excesses of youth. Molecular insights into axonal pruning. Neuron *38*, 849–852.
8. Lee, T., Lee, A., and Luo, L. (1999). Development of the Drosophila mushroom bodies: sequential generation of three distinct types of neurons from a neuroblast. Development *126*, 4065–4076.
9. Larsen, C.W., Hirst, E., Alexandre, C., and Vincent, J.P. (2003). Segment boundary formation in Drosophila embryos. Development *130*, 5625–5635.
10. Technau, G., and Heisenberg, M. (1982). Neural reorganization during metamorphosis of the corpora pedunculata in Drosophila melanogaster. Nature *295*, 405–407.
11. Katzmann, D.J., Odorizzi, G., and Emr, S.D. (2002). Receptor downregulation and multivesicular-body sorting. Nat. Rev. Mol. Cell Biol. *3*, 893–905.
12. Sunio, A., Metcalf, A.B., and Kramer, H. (1999). Genetic dissection of endocytic trafficking in Drosophila using a horseradish peroxidase-bride of sevenless chimera: hook is required for normal maturation of multivesicular endosomes. Mol. Biol. Cell *10*, 847–859.
13. Stocker, R.F., Edwards, J.S., and Truman, J.W. (1978). Fine structure of degenerating abdominal motor neurons after eclosion in the sphingid moth, Manduca sexta. Cell Tissue Res. *191*, 317–331.
14. Younossi-Hartenstein, A., Salvaterra, P.M., and Hartenstein, V.

(2003). Early development of the Drosophila brain: IV. Larval neuropile compartments defined by glial septa. J. Comp. Neurol. *455*, 435–450.

15. Robinow, S., and White, K. (1991). Characterization and spatial distribution of the ELAV protein during Drosophila melanogaster development. J. Neurobiol. *22*, 443–461.
16. Campbell, G., Goring, H., Lin, T., Spana, E., Andersson, S., Doe, C.Q., and Tomlinson, A. (1994). RK2, a glial-specific homeodomain protein required for embryonic nerve cord condensation and viability in Drosophila. Development *120*, 2957–2966.
17. Xiong, W.C., Okano, H., Patel, N.H., Blendy, J.A., and Montell, C. (1994). repo encodes a glial-specific homeo domain protein required in the Drosophila nervous system. Genes Dev. *8*, 981–994.
18. Hosoya, T., Takizawa, K., Nitta, K., and Hotta, Y. (1995). glial cells missing: a binary switch between neuronal and glial determination in Drosophila. Cell *82*, 1025–1036.
19. Jones, B.W., Fetter, R.D., Tear, G., and Goodman, C.S. (1995). glial cells missing: a genetic switch that controls glial versus neuronal fate. Cell *82*, 1013–1023.
20. Freeman, M.R., Delrow, J., Kim, J., Johnson, E., and Doe, C.Q. (2003). Unwrapping glial biology. Gcm target genes regulating glial development, diversification, and function. Neuron *38*, 567–580.
21. Ito, K., Urban, J., and Technau, G.M. (1994). Distribution, classification and development of Drosophila glial cells in the late embryonic and early larval ventral nerve cord. Rouxs Arch. Dev. Biol. *204*, 284–307.
22. Castino, R., Demoz, M., and Isidoro, C. (2003). Destination 'lysosome': a target organelle for tumour cell killing? J. Mol. Recognit. *16*, 337–348.
23. Mullins, C., and Bonifacino, J.S. (2001). The molecular machinery for lysosome biogenesis. Bioessays *23*, 333–343.
24. Sriram, V., Krishnan, K.S., and Mayor, S. (2003). deep-orange and carnation define distinct stages in late endosomal biogenesis in Drosophila melanogaster. J. Cell Biol. *161*, 593–607.
25. Lee, T., Marticke, S., Sung, C., Robinow, S., and Luo, L. (2000). Cell-autonomous requirement of the USP/EcR-B ecdysone receptor for mushroom body neuronal remodeling in Drosophila. Neuron *28*, 807–818.
26. Reddien, P.W., Cameron, S., and Horvitz, H.R. (2001). Phagocytosis promotes programmed cell death in C. elegans. Nature *412*, 198–202.
27. Ronnevi, L.O. (1977). Spontaneous phagocytosis of boutons on spinal motoneurons during early postnatal development. An electron microscopical study in the cat. J. Neurocytol. *6*, 487–504.
28. Berbel, P., and Innocenti, G.M. (1988). The development of the corpus callosum in cats: a light- and electron-microscopic study. J. Comp. Neurol. *276*, 132–156.
29. Sonnenfeld, M.J., and Jacobs, J.R. (1995). Macrophages and glia participate in the removal of apoptotic neurons from the Drosophila embryonic nervous system. J. Comp. Neurol. *359*, 644–652.
30. Cantera, R., and Technau, G. (1996). Glial cells phagocytose neuronal debris during the metamorphosis of the central nervous system in Drosophila melanogaster. Dev. Genes Evol. *206*, 277–280.
31. Tissot, M., and Stocker, R.F. (2000). Metamorphosis in drosophila and other insects: the fate of neurons throughout the stages. Prog. Neurobiol. *62*, 89–111.
32. Kretzschmar, D., and Pflugfelder, G.O. (2002). Glia in development, function, and neurodegeneration of the adult insect brain. Brain Res. Bull. *57*, 121–131.
33. Stoll, G., and Jander, S. (1999). The role of microglia and macrophages in the pathophysiology of the CNS. Prog. Neurobiol. *58*, 233–247.
34. Awasaki, T., and Ito, K. (2004). Engulfing action of glial cells is required for programmed axon pruning during *Drosophila* metamorphosis. Curr. Biol. *14*, this issue, 668–677.